Extraction of Chemical Information of Suspensions using Radiative Transfer Theory to Remove Multiple Scattering Effects: Application to a Model Multi-Component System

Raimundas Steponavičius[1], *Suresh N. Thennadil*[2*]

[1]Merz Court, School of Chemical Engineering and Advanced Materials, Newcastle University, Newcastle upon Tyne, NE1 7RU, United Kingdom; [2] James Weir Building, 75 Montrose Street, Department of Chemical and Process Engineering, University of Strathclyde, Glasgow, G1 1XJ, United Kingdom.

[*]To whom correspondence should be addressed: suresh.thennadil@strath.ac.uk.

RECEIVED DATE

ABSTRACT

The effectiveness of a scatter correction approach based on decoupling absorption and scattering effects through the use of the radiative transfer theory to invert a suitable set of measurements is studied by considering a model multi-component suspension. The method was used in conjunction with partial least squares regression to build calibration models for estimating the concentration of two types of analytes: an absorbing (non-scattering) species and a particulate (absorbing and scattering) species. The performances of the models built by this approach were compared with those obtained by applying

empirical scatter correction approaches to diffuse reflectance, diffuse transmittance and collimated transmittance measurements. It was found that the method provided appreciable improvement in model performance for the prediction of both the types of analytes. The study indicates that as long as the bulk absorption spectra is accurately extracted, no further empirical pre-processing to remove light scattering effects is required.

KEYWORDS: Scatter correction, Multivariate calibration, Near-infrared spectroscopy, Multiple scattering, Radiative transfer equation, Adding-doubling method.

INTRODUCTION

Development of robust and accurate calibration models for predicting analyte concentration in a particulate sample (e.g. powder mixtures, tissue, blood and other suspensions) using near infrared (NIR) spectroscopy poses a significant challenge due to complications arising from the competing effects of absorption and scattering and the nonlinear nature of sample-to-sample variations in scattering. Various empirical [1-6] and semi-empirical [7] approaches to remove scattering effects from spectra can be found in the literature. However, these approaches have not been adequate for situations where the sample-to-sample variations in light scattering are very large. Therefore, approaches based on separating absorption and scattering effects using fundamentals of light propagation are gaining greater impetus in the field of spectroscopic quantitative analysis of highly scattering samples [8-12]. Recently [13], a method for removing multiple scattering effects using the radiative transfer theory in order to improve the performance of multivariate calibration models was proposed and tested on a model two component (polystyrene-water) system. This method consisted of decoupling the absorption and scattering effects by extracting the bulk absorption ($\boldsymbol{\mu_a}$) and scattering ($\boldsymbol{\mu_s}$) using the radiative transfer equation (RTE) and building a Partial least squares (PLS) regression model using $\boldsymbol{\mu_a}$ to predict the concentration of the analyte of interest. Using simulations, it was shown that this approach in theory should not require any additional pre-processing for removing non-chemical variations due to multiple scattering by the

particles in the suspension. However, when the method was applied to a polystyrene-water system to build a model for predicting the concentration of polystyrene particles, two issues arose: (1) Additional pre-processing of the extracted bulk absorption spectra was required to obtain the best performing calibration model with this approach. (2) Calibration built using the total diffuse transmittance ($\mathbf{T_d}$) led to a better performing calibration model. It was argued that the first issue was due to light losses from the sides of the cuvette at low particle concentrations. The second issue was attributed to an effect specific to the two-component system used. Since polystyrene particles absorb and scatter light, changes in photon path length will be correlated to the particle concentrations in a two-component system. This information would be removed by the decoupling step where the bulk absorption spectra ($\boldsymbol{\mu_a}$) are extracted whereas in the diffuse transmittance measurements ($\mathbf{T_d}$), this information is retained. It was argued that this effect is unique to a two-component system and thus when multi-component samples are considered, calibration models built on $\boldsymbol{\mu_a}$ should perform significantly better than when $\mathbf{T_d}$ measurements are used.

In this paper, the effectiveness of this scatter correction approach based on the RTE is evaluated using a model multi-component system. The objectives of this study were (1) to determine if eliminating light losses from the sides of the cuvette will indeed remove the need for additional pre-processing, (2) to evaluate the performance of calibration models built after extracting the bulk absorption spectra for a multi-component suspension for predicting (a) the concentration of a particulate species that absorbs and scatters light and (b) the concentration of a purely absorbing (non-scattering) species.

MATERIALS AND METHODS

Decoupling of scattering and absorption effects

The methodology for estimation of concentrations of chemical components in suspensions considered here consists of two steps namely, decoupling of the scattering and absorption effects using radiative transfer theory and then building the calibration model for estimating the concentration of the analyte of interest using the extracted bulk absorption spectra. The critical step in this methodology is the

decoupling of absorption and scattering effects. This is achieved by inverting an appropriate set of measurements using the radiative transfer equation (RTE) which, for a specific wavelength λ is given by:

$$\frac{d\mathbf{I}(\mathbf{r},\mathbf{s},\lambda)}{d\mathbf{s}} = -\mu_t(\lambda)\cdot\mathbf{I}(\mathbf{r},\mathbf{s},\lambda) + \frac{\mu_s(\lambda)}{4\cdot\pi}\int_{4\pi} p(\mathbf{r},\hat{\mathbf{s}},\lambda)\cdot\mathbf{I}(\mathbf{r},\hat{\mathbf{s}},\lambda)\,d\omega \qquad (1)$$

where $\mathbf{I}(\mathbf{r},\mathbf{s},\lambda)$ is the specific intensity at a distance r from source along the directional vector **s**, $\mu_a(\lambda)$ (cm^{-1}) is the bulk absorption coefficient, $\mu_s(\lambda)$ (cm^{-1}) is the bulk scattering coefficient, $\mu_t(\lambda) = \mu_a(\lambda) + \mu_s(\lambda)$ is the total extinction coefficient, $p(\mathbf{r},\hat{\mathbf{s}},\lambda)$ is the phase function, which is a measure of the angular distribution of scattered light and ω is the solid angle. The phase function is represented as a function of the anisotropy factor g(λ) through the use of Henyey-Greenstein approximation [14] .(see eq. (6) in Ref. 13).

Through the inversion of (1), the parameters $\mu_a(\lambda)$, $\mu_s(\lambda)$ and g(λ) for a sample are obtained from the measurements. This is carried out for all wavelengths at which the measurements are made resulting in a spectrum of these parameters which are denoted as vectors $\boldsymbol{\mu_a}$, $\boldsymbol{\mu_s}$ and **g**. The inversion will then result in the decoupling of absorption and scattering effects with $\boldsymbol{\mu_s}$ and **g** containing the effects due to scattering and $\boldsymbol{\mu_a}$ representing the absorption properties of the sample. Further the bulk absorption is related linearly to the concentration of the individual species present in the sample [13].

In order to extract the bulk optical properties by inverting the RTE, at least three measurements at each wavelength are required. The three measurements used in this study for extraction of the optical properties were: total diffuse transmittance ($\mathbf{T_d}$), total diffuse reflectance ($\mathbf{R_d}$) and collimated transmittance ($\mathbf{T_c}$), the bold letters indicating that these are vectors of measurements at several wavelengths. In this work, an inverse Adding-Doubling algorithm (IAD) was used to extract the bulk

optical parameters [15,16]. The extracted bulk absorption spectra are used for building a multivariate calibration model for estimating the concentration of the chemical component of interest.

EXPERIMENT

Design of Experiments

The model multi-component system constructed for this study was a four-component system consisting of water, deuterium oxide, ethanol and polystyrene particles. The model system was chosen such that we can study the problem of predicting the concentration of an analyte in a suspension for two commonly occurring situations namely, the case where the analyte (a) is an absorbing species and (b) is a species that both absorbs and scatters light (i.e. a particulate species). In this study, the prediction of ethanol concentration will correspond to case (a) and the prediction of the concentration of polystyrene particles will correspond to case (b). By having 4 chemical components, we can ensure that in the dataset collected, the concentrations of the two analytes of interest are not correlated to one another or to other components in the sample.

Ethanol (99.8% purity) was purchased from Fisher Scientific, heavy water (99.9% purity) was purchased from Qmx Laboratories and polystyrene latex suspensions (10% by weight of particles) of different particle sizes were bought from Duke Scientific. The three absorbing components ethanol, water and heavy water are fully miscible and they do not dilute or swell polystyrene particles at the concentrations used in this study

.

There are three variables of interest from the point of view of experimental design for attaining the objectives of this study, namely, ethanol concentration, polystyrene concentration and particle size. The range of particle size and concentration had to be chosen such that the following conditions were satisfied: stable suspension, multiple scattering and sufficient signals in all three measurements. A stability test, during which the change in transmittance was observed in time, revealed that the rate of settlement for polystyrene particles larger than 500 nm is appreciable. Therefore 500nm was chosen as

the upper limit for particle diameter. The highest concentration of particles was set to 5 %wt., beyond which the signal in the transmission mode gets too low for samples with 500 nm diameter particles i.e. we get into the zone of low signal-to-noise ratio and nonlinear detector response. The lower limits for particle size (100nm diameter) and concentration (1% by weight) were chosen so that for the measurement configurations used the light losses through the sides of the cuvette [17-19] were negligible. Five particle sizes of mean diameters 100, 200, 300, 430 and 500 nm, five particle concentrations centered around 1, 2, 3, 4 and 5 %wt. and five concentrations of ethanol centered around 2, 4, 6, 8 and 10 %wt. were used to build a dataset consisting of a total of 44 samples. These were prepared using various combinations of the concentrations of the components and particle sizes in a manner to ensure that in the resulting dataset the correlation between ethanol concentration and the other components and the correlation between polystyrene concentration and the other components were negligible.

Since the number of components is fairly small, it is not possible to get zero correlation between any pair of components because of the closure condition i.e. $\sum_i w_i = 1$ where w_i represents concentration of the i^{th} analyte in the sample expressed as weight fraction. However, the concentrations of the analytes in the dataset can be chosen such that the correlation between the components of interest (ethanol and polystyrene concentrations) and the rest is negligible by allowing the correlation between the components that are not of direct interest for the current study, namely water and deuterated water to be as high as necessary to achieve this goal. The correlation matrix for variables for this dataset is given in Table 1 showing that the correlations involving ethanol and polystyrene concentrations are negligible. Samples were prepared by weighing the actual masses of species added and then calculating the concentrations as % wt. Mass concentrations were then converted into volumetric concentrations for calibration and prediction (the density of water, heavy water, ethanol and polystyrene were taken as 1 kg/m^3, 1.106 kg/m^3, 0.789 kg/m^3 and 1.05 kg/m^3 respectively). Just prior to making the spectroscopic measurements the samples were mildly shaken to ensure that polystyrene particles are uniformly distributed in the sample/suspension. The order of measurements of the samples was randomised to

avoid any possible correlations of the concentrations with experimental conditions (ambient temperature, instrument drift etc.).

Measurement set up

The measurement set up used was the same as the one used in previous studies for extracting bulk optical properties [13,20,21]. Three measurements $\mathbf{T_c}$, $\mathbf{T_d}$ and $\mathbf{R_d}$ were taken for each sample which was placed in a 1mm path length cuvette made of special optical glass (100.099-OS, Hellma) using a scanning spectrophotometer (CARY 5000, Varian Inc.) fitted with a diffuse reflectance accessory (DRA-2500). For this study a fixed spectral bandwidth of 7 nm was used for the whole wavelength region. Spectral data was collected in the wavelength region 1500-1880 nm at 2 nm intervals with an integration time of 10 seconds resulting in measurements at 191 discrete wavelengths per spectrum. This wavelength range was chosen because the first overtone peaks of polystyrene and ethanol due to C-H stretching vibrations occur in this region.

Extraction of bulk optical properties

The inverse adding-doubling (IAD) method [18] was used to extract the bulk optical properties $\boldsymbol{\mu_a}$, $\boldsymbol{\mu_s}$ and $\mathbf{g}$ from the measurements of $\mathbf{T_d}$, $\mathbf{R_d}$, and $\mathbf{T_c}$. The inversion algorithm used the collimated transmittance measurements as a soft constraint as described in [13]. In addition to the measurements and the sample thickness, there are additional inputs required for the inversion. These are the refractive indices of the cuvette, air and the sample. The refractive index of the cuvette was provided by the manufacturer (Hellma) and that of air was taken as 1. The sample refractive index will be dependent on the concentrations of the components in the sample. Thus it would change from sample-to-sample. One way to calculate the refractive index of the sample is to use a weighted sum of the refractive indices of the individual components where the weights are the weight fractions of the components in the sample. However, in practice, for future samples on which the calibration model will be applied these values will not be known. A plausible approach will be to use typical values of refractive index for the mixture. In

this work, since water was the major component, the refractive index of the sample could be set equal to the refractive index of water. The inversion was run with both approaches i.e. using a weighted sum of the refractive index and using just the refractive index of water. The real refractive indices of water, ethanol, polystyrene and the glass of the measurement cell in the chosen wavelength range change little i.e.: from 1.3121 to 1.2993, from 1.3540 to 1.3535, from 1.5558 to 1.5529 and from 1.507 to 1.5027 respectively over the wavelength range considered. The refractive indices of ethanol and heavy water were taken from the refractive index database available [22].

Calibration

Multivariate calibration was carried out using PLS regression. The performance of the PLS models were evaluated using root mean square error of cross validation (RMSECV). Cross validation was carried out using the 'leave-one-out' method. Further, all the raw spectra were smoothed using Savitsky-Golay filter with the window width 9 and the polynomial order 3 to remove noise in the measurements. For all models, the spectra were mean-centered. The computations were carried out using Matlab® and the PLS models were built using PLS_Toolbox by Eigenvectors Research Inc.

RESULTS AND DISCUSSION

The three measurements (diffuse reflectance, diffuse transmittance and collimated transmittance) and the extracted bulk absorption spectra for the samples are presented in figure 1. It is seen that the magnitudes of variation in the dataset are much larger in the measurements (diffuse reflectance, diffuse transmittance and collimated transmittance) than in the extracted μ_a where the variations due to multiple light scattering have been removed. However, there is still some "spread" in the data which is due to the fact that that while μ_a represents the absorption properties of the sample, it still contains a contribution from the particulate species which are particle-size dependent. Compared to the polystyrene-water system that was considered in Ref. 12, the spread in this multi-component data is much larger because the range of particle concentrations spanned in the current study is twice as large.

An important point to note in figure 1 is the broad peak in the wavelength region 1600-1750 nm centered around 1670nm which can be seen most clearly in figures 1 (b) and (d). This peak does not appear in the absorption spectra of the pure components. This indicates that the absorption spectra of the mixtures for the range of concentrations considered here are not additive and that a new absorption peak may be forming due to interactions. To find out which of the components interacted to form this new peak different binary mixtures, namely, ethanol-water, ethanol-D_2O and water-D_2O, were examined. It was found that spectra of H_2O – D_2O mixtures exhibited this peak. It appears neither in the absorption spectrum of pure water nor in the absorption spectrum of deuterium oxide. Figure 2(a) shows the spectra of H_2O – D_2O mixtures of different composition. The peaks centered around 1450, 1790 and 1900 nm are the first overtones of O–H (from H_2O), while a comparatively weak and broad band of O–D (from D_2O) is seen centered approximately around 1600nm. Figure 2(b) shows the absorbance at 3 different wavelengths: 1670 nm which is approximately the centre of the broad peak in the 1600-1750 nm and 1500 nm and 1800 nm which lie on either side of this peak. At the latter wavelengths which include absorption due to both O-H and O-D overtones, the absorption changes linearly with concentration of water. The absorbance at 1670nm increases as the ratio of D_2O to H_2O is increased and then drops when the % vol. of water becomes greater than about 55-60% by volume reaching the value of absorbance of pure water at 100% by volume. As indicated in the figure, the absorbance at this wavelength is non-linear with the points being fitted well with a second order polynomial with respect to the water concentration. This suggests that the peak is probably due to the formation of H_2O – D_2O dimers. Studies of water, D_2O and HDO dimers have been extensively carried out in the past by researchers[23-27] which have shown that dimers with H_2O.DOD and D_2O.HOH structures are formed with the dimer preferring the former structure [23,24]. From the point of view of building a PLS model for predicting analyte concentrations in this model system, this effect will manifest itself as an extra latent variable (LV) in a calibration model for analyte concentrations.

(a) Prediction of concentration of absorbing-only (non-scattering) species

In the model four-component system considered in this study, ethanol corresponds to an absorbing-only species as the analyte of interest. In the wavelength region considered, the first overtone bands of ethanol are found at around 1680nm (C-H), 1684nm and 1692nm ($C-H_3$) and bands due to asymmetric vibrations of CH_2 and CH_3 at around1714nm and 1719nm[28]. Calibration models were built using PLS regression both with and without applying pre-processing. The following pre-processing methods were tried: multiplicative scatter correction, standard normal variate, extended multiplicative scatter correction and first and second derivatives. Only the results for pre-processing method that provided the best performing model for each of the measurement set are reported here along with the performance of the corresponding model built without pre-processing. Figure 3(a) shows the RMSECV curves for the models built using different data sets i.e. $\mathbf{T_d}$, $\mathbf{R_d}$, $\mathbf{T_c}$ and $\boldsymbol{\mu_a}$. As mentioned earlier, the bulk absorption spectra $\boldsymbol{\mu_a}$ were extracted using two different values for the refractive index of the sample. In figure 3(a), the curve labeled μ_a denotes the RMSECV curve for the model built with $\boldsymbol{\mu_a}$ extracted by taking the sample refractive index to be the weighted sum of the refractive indices of the individual components in the sample. The curve labeled 'μ_a using $n_{s,w}$' denotes the model built with $\boldsymbol{\mu_a}$ extracted by approximating the refractive index of the samples to be that of pure water. It can be seen from figure 3(a) and Table 2 that the differences in the results are negligible indicating that approximating the refractive index of the sample with that of pure water will not adversely affect the final results. It can be seen that the best results are obtained by using $\boldsymbol{\mu_a}$ without pre-processing with an RMSECV of 0.47 vol% using a PLS model having six latent variables. Since there are 4 components in the samples plus the effect due to the formation of H_2O-D_2O dimers and the effect of particle sizes, this is the number of latent variables that would be expected if the large non-linearities arising from photon path length variations due to multiple scattering have been removed. Predicted versus actual values of ethanol concentration for the best PLS model i.e. the one built on $\boldsymbol{\mu_a}$, are plotted in figure 3(b). Note that the RMSECV obtained using collimated transmittance ($\mathbf{T_c}$) measurements also is the same as that obtained when using $\boldsymbol{\mu_a}$ though it leads to a model with 10 latent variables compared to 6 for the model built on $\boldsymbol{\mu_a}$. The low RMSECV for

the model using $\mathbf{T_c}$ is not surprising since this measurement contains largely unscattered light at low particle concentrations. As the particle concentration increases, this measurement will be increasingly contaminated with scattered light as well as facing a rapid reduction in signal-to-noise. At moderate to high concentrations this measurement will not be feasible due to lack of sufficient signal and other configurations such as diffuse reflectance or diffuse transmittance measurements will have to be used.

It is seen that for diffuse transmittance and diffuse reflectance data, empirical pre-processing can lead to appreciable drop in RMSECV compared to building a model without any pre-processing. The best pre-processing method for these data among the ones considered was the version of extended multiplicative scatter correction method (EMSCL) which models wavelength dependence as a logarithmic function [2].

(b) Prediction of concentration of scattering-absorbing (particulate) species

In the model system considered in this study, polystyrene latex particles correspond to a scattering-absorbing species as the analyte of interest. In the wavelength range considered, first overtone peaks of polystyrene are centered around 1680nm (C-H). Figure 4(a) shows the RMSECV curves for the models built using different data sets i.e. $\mathbf{T_d}$, $\mathbf{R_d}$, $\mathbf{T_c}$ and $\boldsymbol{\mu_a}$. Table 3 summarizes the performance of the models. As in the case with absorbing-only species, the best performance was achieved by the model built on the extracted bulk absorption spectra $\boldsymbol{\mu_a}$. In this case one more latent variable than that required for the absorbing-only case was needed i.e. 7 latent variables were needed. The increase could be due to a small amount of particle concentration dependent scattering effect being embedded in the extracted $\boldsymbol{\mu_a}$. Predicted versus actual values of polystyrene concentration for the best PLS model i.e. the one built on $\boldsymbol{\mu_a}$, are plotted in figure 4 (b).

As mentioned earlier, for the two component (polystyrene-water) system studied in an earlier work [13], the model built using $\mathbf{T_d}$ performed much better than the one built on $\boldsymbol{\mu_a}$. It was hypothesized that this result was due to the secondary correlations existing between the polystyrene concentration and photon path lengths which was removed when extracting $\boldsymbol{\mu_a}$. Since in a multi-component system this correlation

would not exist, it was predicted that there will be degradation in the performance of models built on $\mathbf{T_d}$ for estimating particle concentrations in such a system compared to using $\boldsymbol{\mu_a}$. The result reported here confirms this hypothesis.

Again, no significant difference is observed between the two different values used for the refractive index of sample, suggesting that not accounting for the small changes in refractive index due to variations in the composition of the samples will not adversely affect the performance of the calibration models built using $\boldsymbol{\mu_a}$ extracted by inverting the radiative transfer equation.

Comparing the results in predicting the two types of species i.e. the absorbing and the scattering-absorbing species, using the empirically pre-processed measurements, one can notice that in the first case a better performance was obtained using $\mathbf{R_d}$ pre-processed with EMSCL and in the second case using $\mathbf{T_d}$ pre-processed with EMSCL.

CONCLUSIONS

Through the use of a model multi-component system, this study demonstrates the effectiveness of decoupling the scattering and absorption effects using the radiative transfer equation in appreciably improving the performance of multivariate calibration models for particulate systems for two commonly occurring situations namely when the analyte of interest is an absorbing species which does not scatter light and when the analyte of interest is a absorbing species which scatters light i.e. it is a particle. The study indicates that as long as the bulk absorption spectra are accurately extracted, no further empirical pre-processing to remove light scattering effects is required. In this study the required set of measurements for this purpose was obtained using an integrating sphere setup and the use of the adding-doubling method for solving the radiative transfer equation. The range of concentrations that can be studied is limited by light losses that are not accounted for by the adding-doubling method as well as the signal that will be available in the transmission mode at high particle concentrations. The first issue could be addressed by the use of monte carlo simulations to solve the radiative transfer equation so that light losses can be taken into account. The second issue can be addressed by considering alternative sets

of measurements such as spatially resolved measurements where reflectances from the sample at different distances from the incident beam are collected.

ACKNOWLEDGMENT

This work was funded through Marie Curie FP6 (INTROSPECT) and EPSRC grants GR/S50441/01 and GR/S50458/01.

LIST OF FIGURES

LIST OF TABLES

Table 1. Correlation matrix between variables (concentrations of analytes and particle diameters) in the dataset.

Variable	Ethanol Concentration	Polystyrene Concentration	Particle Diameter	Water Concentration	D_2O Concentration
Ethanol Concentration	**1.00**	0	0	0.14	0.12
Polystyrene Concentration	0	**1.00**	0	0.09	0.04
Particle Diameter	0	0	**1.00**	0.26	0.26
Water Concentration	0.14	0.09	0.26	**1.00**	0.96
D_2O Concentration	0.12	0.04	0.26	0.96	**1.00**

Table 2. Performance of calibration models for estimating concentration of absorbing-only species (ethanol).

Data	Pre-processing	LVs	RMSECV (% vol.)
$\mathbf{R_d}$	None	7	0.94
	EMSCL	5	0.63
$\mathbf{T_d}$	None	5	1.83
	EMSCL	8	0.81
$\mathbf{T_c}$	None	10	0.48
$\boldsymbol{\mu_a}$	None	6	0.48
$\boldsymbol{\mu_a}$ using $n_{s,w}$	None	6	0.47

Table 3. Performance of calibration models for estimating concentration of scattering-absorbing species (polystyrene).

Data	Pre-processing	LVs	RMSECV (% vol.)
$\mathbf{R_d}$	None	7	0.52
	EMSCL	5	0.57
$\mathbf{T_d}$	None	7	0.76
	EMSCL	7	0.43
$\mathbf{T_c}$	None	7	0.47
$\boldsymbol{\mu_a}$	None	7	0.31
$\boldsymbol{\mu_a}$ using n_{sw}	None	7	0.31

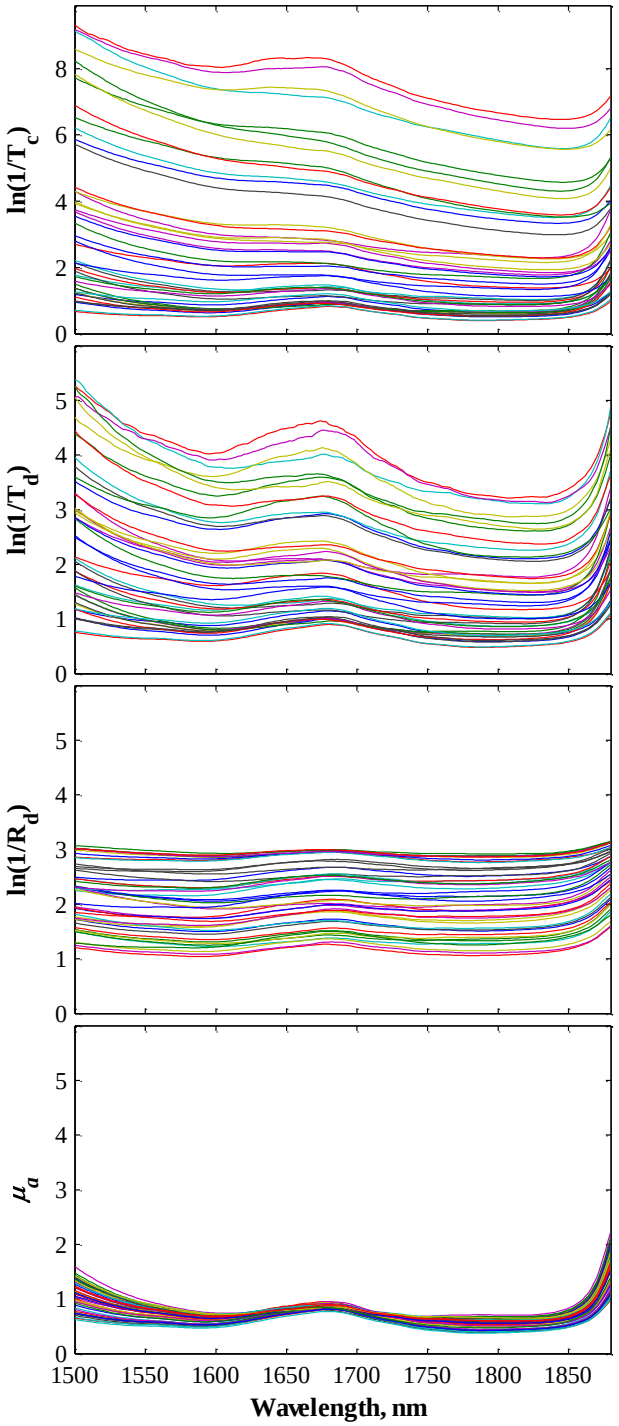

Figure 1. Collimated transmittance, total transmittance, total reflectance and bulk absorption spectra of the 4 component model system for different compositions.

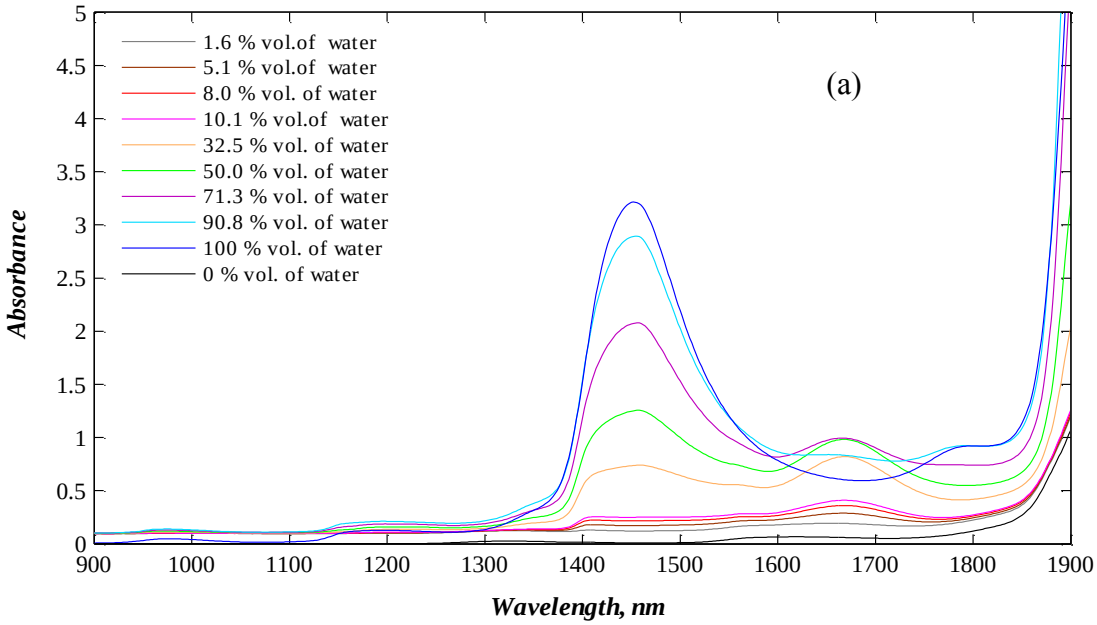

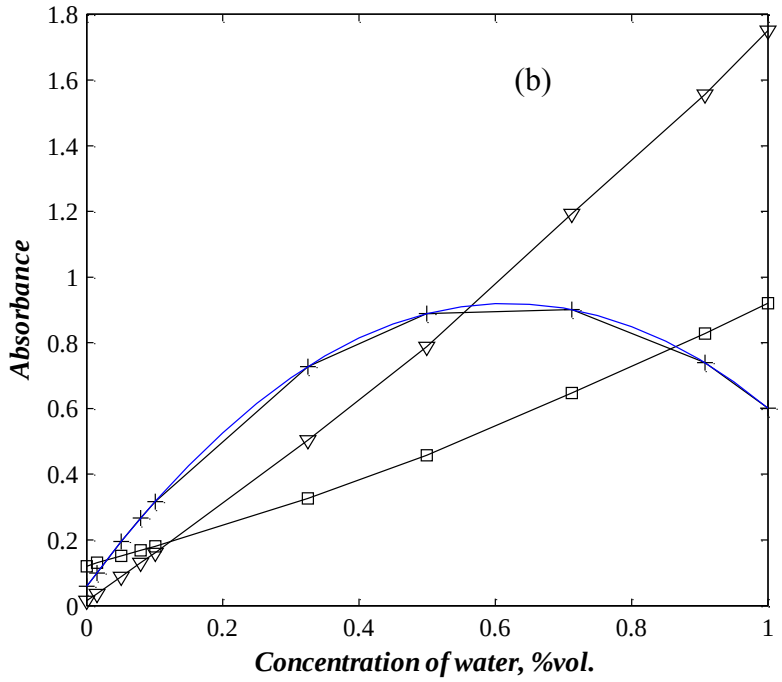

Figure 2. (a) Absorption spectra of H_2O-D_2O mixtures; (b) Dependence of absorption on H_2O-D_2O composition: 1500 nm (triangle), 1880 nm (square) and 1670 nm (cross); the blue line is the fit.

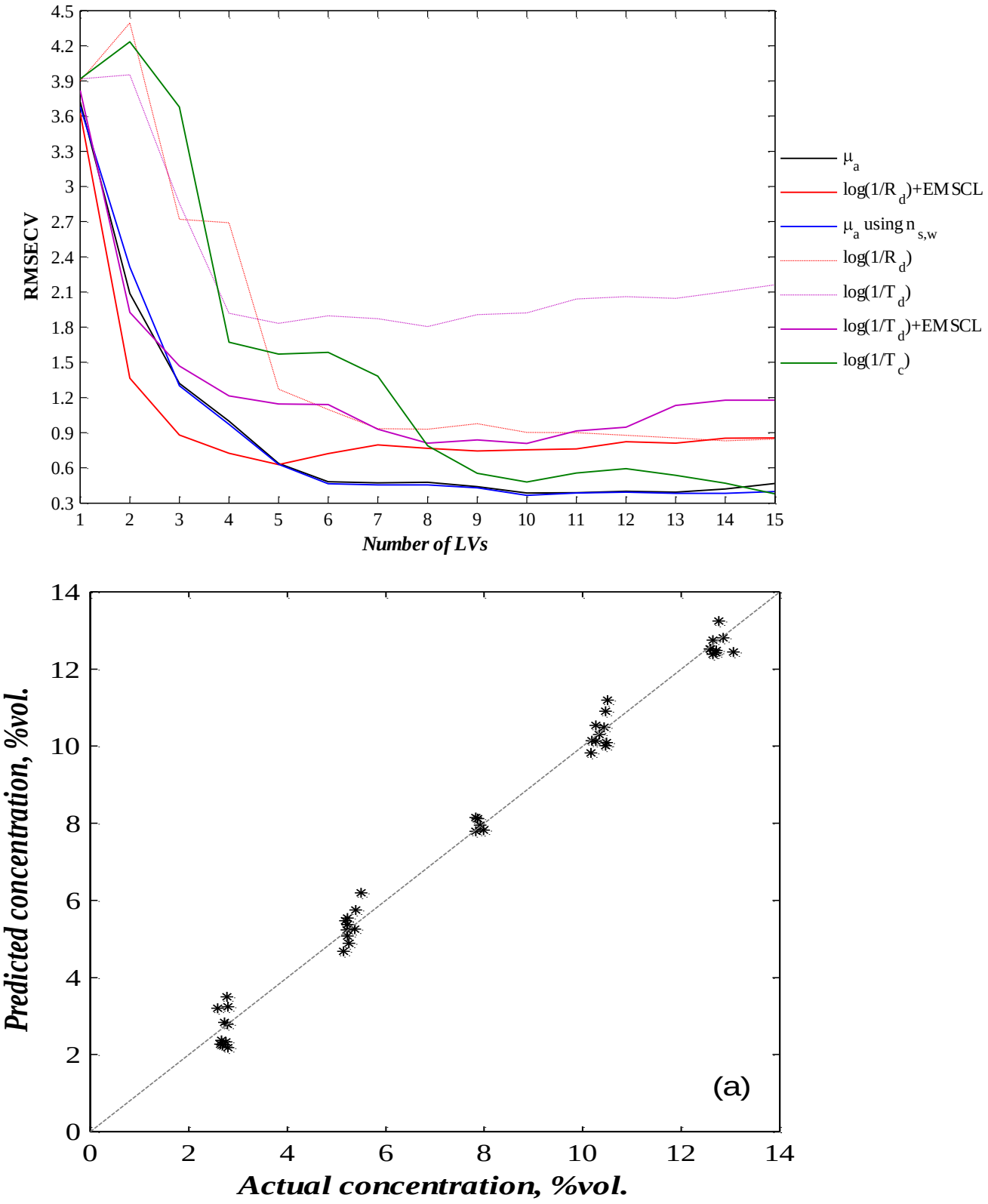

Figure 3. (a) RMSECV curves for prediction of ethanol concentration; (b) Predicted versus actual values of ethanol concentration.

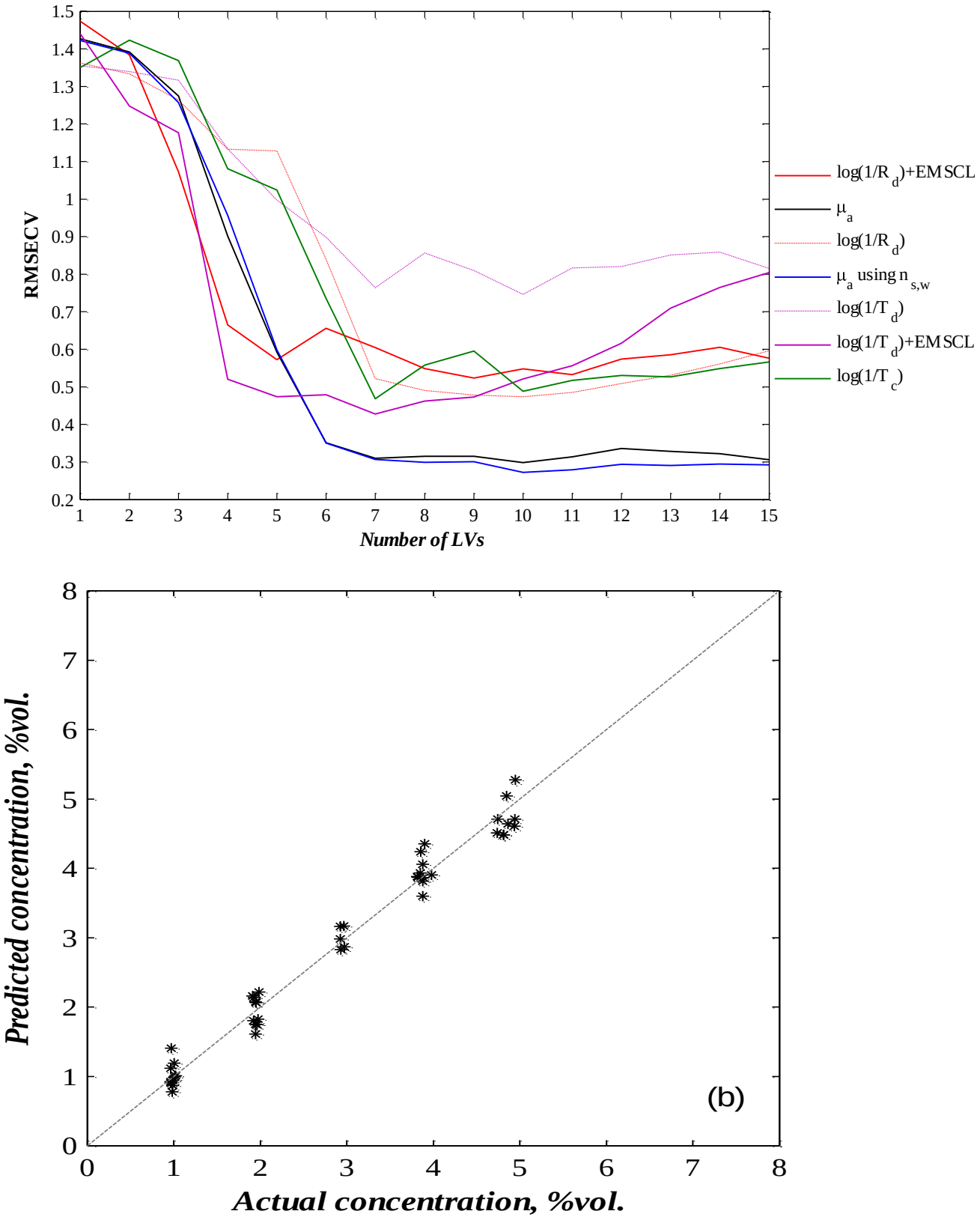

Figure 4. (a) RMSECV curves for prediction of concentration of polystyrene particles; (b) Predicted versus actual values of concentration of polystyrene.

REFERENCES

(1) Martens, H.; Nielsen, J. P.; Engelsen, S. B. Analytical Chemistry 2003, 75, 394-404.

(2) Thennadil, S. N.; Martin, E. B. Journal of Chemometrics 2005, 19, 77-89.

(3) Chen, Z. P.; Morris, J.; Martin, E. Analytical Chemistry 2006, 78, 7674-7681.

(4) Helland, I. S.; Naes, T.; Isaksson, T. Chemometrics and Intelligent Laboratory Systems 1995, 29, 233-241.

(5) Rinnan, A.; van den Berg, F.; Engelsen, S. B. Trac-Trends in Analytical Chemistry 2009, 28, 1201-1222.

(6) Svensson, O.; Kourti, T.; MacGregor, J. F. Journal of Chemometrics 2002, 16, 176-188.

(7) Thennadil, S. N.; Martens, H.; Kohler, A. Applied Spectroscopy 2006, 60, 315-321.

(8) Leonardi, L.; Burns, D. H. Applied Spectroscopy 1999, 53, 628-636.

(9) Abrahamsson, C.; Johansson, J.; Andersson-Engels, S.; Svanberg, S.; Folestad, S. Analytical Chemistry 2005, 77, 1055-1059.

(10) Chaiken, J.; Goodisman, J. Journal of Biomedical Optics 2010, 15, 037007.

(11) Leger, M. N. Applied Spectroscopy 2010, 64, 245-254.

(12) Ottestad, S.; Isaksson, T.; Saeys, W.; Wold, J. P. Applied Spectroscopy 2010, 64, 795-804.

(13) Steponavicius, R.; Thennadil, S. N. Analytical Chemistry 2009, 81, 7713-7723.

(14) Ishimaru, A. Wave propagation and scattering in random media; IEEE Press: New York, USA, 1997.

(15) Prahl, S. A. In Optical-thermal response of laser irradiated tissue; Welch, A. J., van Gemert, M. J. C., Eds.; Plenum Press: New York, 1995, p 101-129.

(16) Van de Hulst, H. C. Multiple light scattering: tables formulas and applications; USA Academic: USA, 1980; Vol. 1.

(17) de Vries, G.; Beek, J. F.; Lucassen, G. W.; van Gemert, M. J. C. Ieee Journal of Selected Topics in Quantum Electronics 1999, 5, 944-947.

(18) Prahl, S. A.; Vangemert, M. J. C.; Welch, A. J. Applied Optics 1993, 32, 559-568.

(19) Zhu, D.; Lu, W.; Zeng, S. Q.; Luo, Q. M. Journal of Biomedical Optics 2007, 12.

(20) Dzhongova, E.; Harwood, C. R.; Thennadil, S. N. Applied Spectroscopy 2009, 63, 25-32.

(21) Saeys, W.; Velazco-Roa, M. A.; Thennadil, S. N.; Ramon, H.; Nicolai, B. M. Applied Optics 2008, 47, 908-919.

(22) Refractive index database available at http://refractiveindex.info

(23) Devlin, J. P. Journal of Chemical Physics 2000, 112, 5527-5529.

(24) Engdahl, A.; Nelander, B. The Journal of Chemical Physics 1987, 86, 1819-1823.

(25) Worley, J. D.; Klotz, I. M. The Journal of Chemical Physis 1966, 45, 2868 - 2871.

(26) Thomas, M. R.; Scheraga, H. A.; Schrier, E. E. The Journal of Physical Chemistry 1965, 69, 3722 - 3726.

(27) Lappi, S. E.; Smith, B.; Franzen, S. Spectrochimica Acta Part A 2004, 60, 2611 - 2619.

(28) Engelhard, S.; Lohmannsroben, H.; Schael, F. Applied Spectroscopy 2004, 58, 1205 - 1209.

FOR TOC ONLY

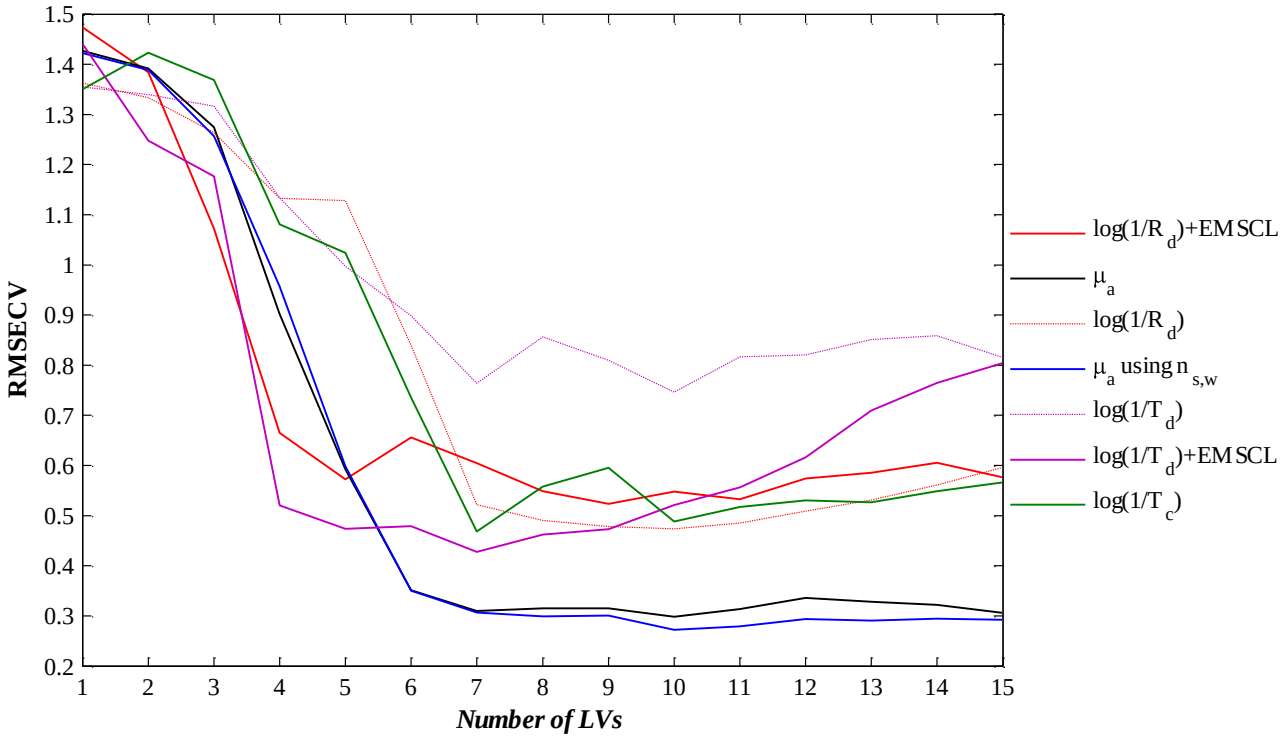
RMSECV
Number of LVs
log(1/R d)+EMSCL
μa
log(1/R d)
μa using n s,w
log(1/T d)
log(1/T d)+EMSCL
log(1/T c)